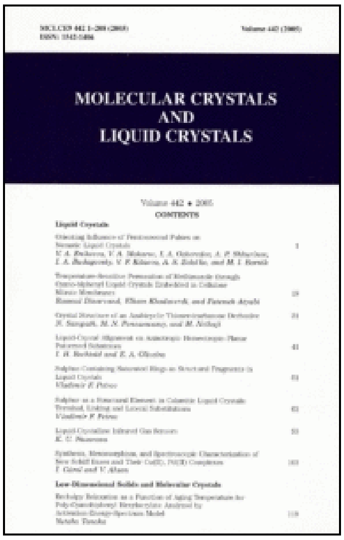

Molecular Crystals and Liquid Crystals
Publication details, including instructions for authors and subscription information:
http://www.informaworld.com/smpp/title~content=t713644168

Molecular and Crystal Structure, Spectroscopic Properties of N-[4-(3-Methyl-3-Phenyl-Cyclobutyl)-Thiazol-2-yl]-N'-(1*H*-Pyrrol-2-Ylmethylene)-Hydrazine by Experimental Method and Quantum Chemical Calculation

Çiğdem Yüksektepe[a]; Hanife Saraçoğlu[b]; Nezihe Çalışkan[c]; Ibrahim Yilmaz[d]; Alaaddin Cukurovali[e]
[a] Department of Physics, Faculty of Science, Cankiri Karatekin University, Ballica, Cankiri, Turkey [b] Department of Physics Education, Faculty of Education, Ondokuz Mayis University, Kurupelit, Samsun, Turkey [c] Department of Physics, Faculty of Arts and Sciences, Ondokuz Mayis University, Kurupelit, Samsun, Turkey [d] Department of Chemistry, Faculty of Science, Karamanoglu Mehmetbey University, Karaman, Turkey [e] Department of Chemistry, Faculty of Science, Firat University, Elazig, Turkey

To cite this Article Yüksektepe, Çiğdem , Saraçoğlu, Hanife , Çalışkan, Nezihe , Yilmaz, Ibrahim and Cukurovali, Alaaddin(2010) 'Molecular and Crystal Structure, Spectroscopic Properties of N-[4-(3-Methyl-3-Phenyl-Cyclobutyl)-Thiazol-2-yl]-N'-(1*H*-Pyrrol-2-Ylmethylene)-Hydrazine by Experimental Method and Quantum Chemical Calculation', Molecular Crystals and Liquid Crystals, 533: 1, 126 — 140

To link to this Article: DOI: 10.1080/15421406.2010.504655

URL: http://dx.doi.org/10.1080/15421406.2010.504655

Mol. Cryst. Liq. Cryst., Vol. 533: pp. 126–140, 2010

ISSN: 1542-1406 print/1563-5287 online
DOI: 10.1080/15421406.2010.504655

Molecular and Crystal Structure, Spectroscopic Properties of N-[4-(3-Methyl-3-Phenyl-Cyclobutyl)-Thiazol-2-yl]-N′-(1*H*-Pyrrol-2-Ylmethylene)-Hydrazine by Experimental Method and Quantum Chemical Calculation

ÇIĞDEM YÜKSEKTEPE,[1] HANIFE SARAÇOĞLU,[2]
NEZIHE ÇALIŞKAN,[3] IBRAHIM YILMAZ,[4] AND
ALAADDIN CUKUROVALI[5]

[1]Department of Physics, Faculty of Science, Cankiri Karatekin University, Ballica, Cankiri, Turkey
[2]Department of Physics Education, Faculty of Education, Ondokuz Mayis University, Kurupelit, Samsun, Turkey
[3]Department of Physics, Faculty of Arts and Sciences, Ondokuz Mayis University, Kurupelit, Samsun, Turkey
[4]Department of Chemistry, Faculty of Science, Karamanoglu Mehmetbey University, Karaman, Turkey
[5]Department of Chemistry, Faculty of Science, Firat University, Elazig, Turkey

A new compound ($C_{19}H_{20}N_4S$) *has been synthesized and characterized by* ^1H *nuclear magnetic resonance (NMR),* ^{13}C *NMR, infrared (IR) and ultraviolet (UV)-visible spectroscopy, elemental analysis, and single crystal X-ray diffraction. The compound crystallizes in the triclinic space group P-1. The crystal structure is stabilized by N–H…N intermolecular hydrogen bonding. The optimized molecular geometry, vibrational frequencies, atomic charge distribution, and total energies of the title compound in the ground state have been calculated by using an ab initio method. A density functional theory (B3LYP) method with basis sets 6-311 G (d, p) and 6-31 G (d, p) was used in the calculations. Calculated frequencies and geometrical parameters are in good agreement with the corresponding experimental data. UV-Vis absorption spectra of the compound have been ascribed to their corresponding molecular structure and electrons orbital transitions. In addition, molecular electrostatic potential and thermodynamic parameters of the title compound were determined by the theoretical methods.*

Keywords Crystal structure; hydrazone; quantum Chemical calculation; thiazole

---

Address correspondence to Çiğdem Yüksektepe, Department of Physics, Faculty of Science, Cankiri Karatekin University, TR-18100, Ballica, Cankiri, Turkey. E-mail: yuksekc@yahoo.com

Introduction

Schiff bases constitute an interesting class of chelating agents, capable of coordination with one or more metal ions to form mononuclear as well as polynuclear metal complexes [1,2]. Some of their applications can be found in analytical chemistry and serve as biochemical models [3,4]. Most Schiff bases have antibacterial, anticancer, anti-inflammatory and antitoxic activities [5]; in particular, sulfur-containing Schiff bases are very effective. Hydrazone derivatives have been synthesized in order to investigate the relationship between structure and biological activity [6–8]. Hydrazine has been reported to methylate DNA [9] and interfere in the urea cycle, with the result that citrulline levels are raised in the livers of experimental animals [10,11]. Substituted hydrazines have also found many scientific and commercial applications [12,13]. Hydrazones have been utilized for the determination of carbonyl compounds [14,15]. The thiazole ring is known to be a part of vitamin B1, cocarboxylase, and the cyclic system of penicillin [16]. Thiazole itself and its derivatives are of importance in biological systems as anti-inflammatory, and analgesic agents and inhibitors on lipoxygenase activities [17,18]. Taking into account the above observations, this compound has been synthesized as a part of our ongoing biological active compounds research program [19].

In this work, we report molecular and crystal structure with the formula, $C_{19}H_{20}N_4S$, (I) of the new synthesized hydrazone derivative by a complex of the physical and chemical methods including IR and UV spectroscopy and X-ray single-crystal analysis. In addition the molecular geometry, vibrational spectra, and frontier molecular orbital properties as well as the Mulliken charge distribution of the atoms of this compound were determined using density functional theory (DFT/B3LYP) with 6–311 G (d, p) and 6–31 G(d, p) basis sets. The initial geometry of the compound for all calculations was taken from X-ray refinement data. The results from both experimental and theoretical calculations are compared and the computed geometrical, and spectroscopic parameters are in good agreement with the experimental results.

Experiment

Synthesis of Compound N-[4-(3-Methyl-3-Phenyl-Cyclobutyl)-Thiazol-2-yl]-N′-(1H-Pyrrol-2-Ylmethylene)-Hydrazine

The compound was synthesized as in Scheme 1 by the following procedure. To a solution of hydrazone derivative (**A**) (1.6822 g, 10 mmol) in 50 mL of ethanol, a solution of 1-methyl-1-phenyl-3-(2-chloro-1-oxoethyl) cyclobutane (2.2271 g, 10 mmol) in 20 mL of absolute ethanol was added. After the addition of the α-haloketone, the temperature was raised to 323–328 K and kept at this temperature for 2 h. The solution was cooled to room temperature and then made alkaline with an aqueous

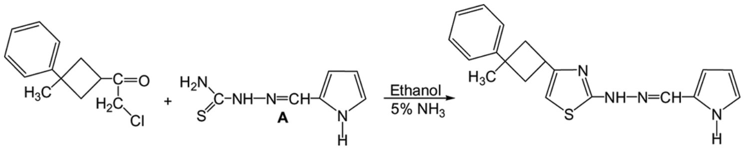

Scheme 1. Synthetic pathway for the synthesis of the target compound (**1**).

solution of NH_3 (5%). The resultant black precipitate was separated by suction, washed with aqueous NH_3 solution several times, and dried in air. A suitable single crystal for crystal structure determination was obtained by slow evaporation of its ethanol solution. Yield: 68%, melting point: 454 K. Characteristic ^1H NMR shifts (acetone-d_6, δ, ppm): 1.53 (s, 3H, -CH_3 on cyclobutane), 2.36–2.41 (m, 2H, -CH_2-cyclobutane), 2.53–2.61 (m, 2H, -CH_2- cyclobutane), 2.90 (brs, 1H, -NH-, D_2O exchangeable), 3.60 (q, $j = 8.78$ Hz, 1H, >CH- cyclobutane), 6.14–6.18 (m, 1H, aromatics), 6.32 (s, 1H, =CH-S, in thiazole), 6.37–6.41 (m, 1H, aromatics), 6.92–6.95 (m, 1H, aromatics), 7.14–7.23 (m, 3H, aromatics), 7.29–7.36 (m, 2H, aromatics), 7.96 (s, 1H, -N=CH- azomethine), 10.55 (brs, 1H, -NH-, D_2O exchangeable). Characteristic ^{13}C NMR shifts (acetone-d_6, δ, ppm): 168.20, 156.06, 152.70, 134.22, 127.82, 127.67, 125.13, 124.64, 121.24, 111.82, 109.11, 101.06, 40.27, 38.34, 30.77, 29.48. Elemental analysis: Calc. for ($C_{19}H_{20}N_4S$): C: 67.83, H: 5.99, N: 16.65; found: C: 67.74, H: 6.04, N: 16.83.

Measurement

IR spectra were recorded on an ATI Unicam-Mattson 1000 FT-IR spectrophotometer using KBr pellets. ^1H nuclear magnetic resonance (NMR) and ^{13}C NMR spectra were obtained by using Bruker 300-MHz and 75-MHz-spectrometers. The ultraviolet (UV) spectra of the compound were determined on a Schimadzu UV-1700 spectrometer in $CHCl_3$ solvent.

X-Ray Crystallography

Data collection was performed at 293 K on a Stoe-IPDS-2 diffractometer equipped with a graphite monochromated Mo-K_α radiation ($\lambda = 0.71073$ Å). The structure was solved by direct methods using SHELXS-97 and refined by a full-matrix least-squares procedure using the program SHELXL-97 [20] (molecular graphics: ORTEP-3 and PLATON for Windows [21, 22]). All nonhydrogen atoms were easily found from the difference Fourier map and refined anisotropically. All hydrogen atoms were included using a riding model and refined isotropically with C–H = 0.93 – 0.97 Å and N–H = 0.86 Å. $U_{iso}(H) = 1.2U_{eq}(C, N)$, $U_{iso}(H) = 1.5U_{eq}$ (for methyl group).

Calculations

Starting geometries of compound (**1**) were taken from X-ray refinement data. The molecular structures of the title compound ($C_{19}H_{20}N_4S$) in the ground state *(in vacuo)* were optimized by DFT methods to include correlation corrections with the 6–311 G (d, p) and 6–31 G (d, p) basis sets. In DFT calculations, hybrid functionals are also used, including the Becke's three-parameter functional (B3) [23], which defines the exchange functional as the linear combination of Hartree-Fock, local, and gradient-corrected exchange terms. The B3 hybrid functional was used in combination with the correlation functionals of Lee et al. [24]. Two sets of vibrational frequencies, Mulliken charges, and lowest unoccupied molecular orbital (LUMO) - highest occupied molecular orbital (HOMO) energy differences for these species were calculated with this method. All the calculations were performed using the Gaussview molecular visualization program [25] and Gaussian 03 program on a personal computer [26].

Result and Discussion

Description of the Crystal Structure

Details of crystal parameters, data collection, structure solution, and refinement are given in Table 1. The title compound contains thiazole, hydrazone, phenyl, pyrrol, and cylobutane moieties. The crystal structure with the formula, $C_{19}H_{20}N_4S$, (I) is shown in Fig. 1. The central five-member thiazole ring is essentially planar, to within 0.0048 Å. The dihedral angles between the phenyl ring (C1 through C6), cyclobutane ring, pyrrol ring, and thiazole ring are equal to 88.53(5)°, 55.44(8)°, and 24.06(10)°, respectively. Only some of bond distances in the thiazole ring show partial double-bond character so that C12–N1, S1–C13, and S1–C14 bond distances of 1.397(2), 1.721(2), 1.731(2) Å show the values of single-bond character (Table 2). The S–C bond distances are shorter than the accepted value for an S-C sp^2 single bond with 1.76 Å [27]. It is worth noting that the C14–N1 bond distance value of

Table 1. Crystallographic data of (**1**)

Empirical Formula	$C_{19}H_{20}N_4S$
Molecular weight	336.5
Temperature, T (K)	296
Wavelength (Å)	0.71073
Crystal system	Triclinic
Crystal size (mm^3)	0.520 × 0.497 × 0.250
Space group	P-1
a (Å)	5.8448 (5)
b (Å)	10.2622 (9)
c (Å)	14.5289 (11)
α (°)	88.693 (7)
β (°)	85.035 (6)
γ (°)	87.919 (7)
Volume, V (Å^3)	867.44 (5)
Z	2
T_{min}, T_{maks}	0.9064, 0.9552
Calculated density (Mg m^{-3})	1.29
θ range (°)	1.99–27.07
Index ranges	$H = -6 \rightarrow 6$, $k = -12 \rightarrow 12$, $l = -17 \rightarrow 17$
Measured reflections	7,160
Independent reflections	3,036
Observed reflections ($I > 2\sigma$)	2,516
Goodness-of-fit on F^2	1.050
R_1 indice ($I > 2\sigma$)	0.036
wR_2 indice ($I > 2\sigma$)	0.095

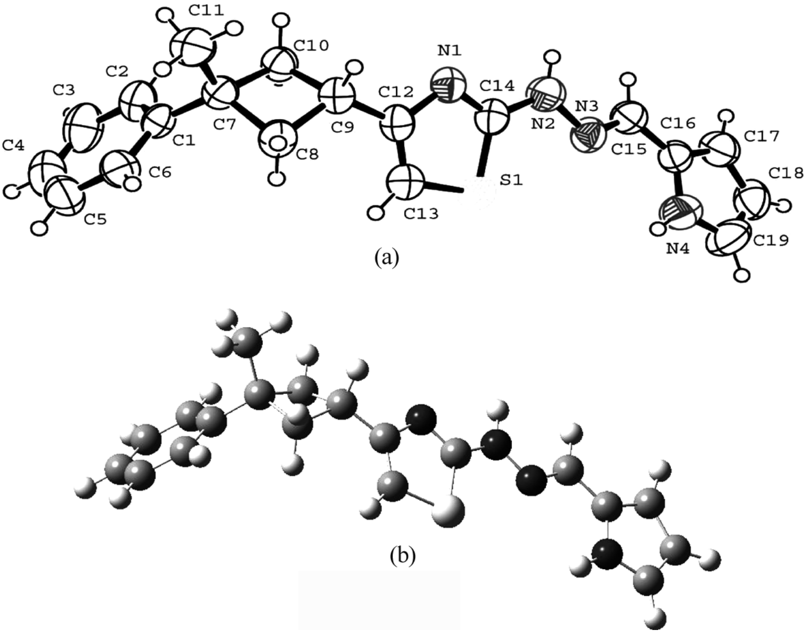

Figure 1. (a) ORTEP drawing of the basic crystallographic unit showing the atom-numbering scheme. Displacement ellipsoids are drawn at the 50% probability level and all H atoms are shown as small spheres of arbitrary radii. (b) Gaussview drawing of the title compound.

1.302(2) Å falls in the C=N double-bond distance region and is shorter than the C=N double-bond distance found in the related thiazole ring structure [28]; also, in the thiazole ring the C12–C13 bond distance of 1.342(3) Å shows the value of C=C double-bond character.

The thiazole and pyrrol rings are linked by the strictly planar N2–N3 = C15–C16 fragment and its torsion angle is 176.66(14)°. In the hydrazone group, the C15–N3 double-bond distance of 1.268(2) Å is shorter than the C=N bond distance found in related hydrazone structures; that is, 1.2810(19) Å in Liu et al. [29] and 1.272(2) Å Ma et al. [30]. The steric interaction between the substituent groups on the cyclobutane ring means that this ring deviates significantly from planarity. Literature values for the puckering of the cyclobutane ring are 29.03(13)° in Yüksektepe *et al.* [31] and 26.8(2)° in Yüksektepe *et al.* [32]. In this article, the C8/C9/C10 plane forms a dihedral angle of 23.49(13)° with the C10/C7/C8 plane.

In the crystal packing, the molecules are linked head to head by N–H…N hydrogen bonding. In this hydrogen bonding, the atom N2 at (x, y, z) acts as a donor to atom N1 at (1 −x, 1 − y, 1 − z), generating a centrosymmetric $R_2^2(8)$ rings centered at (1/2, 1/2, 1/2). The $R_2^2(8)$ rings formed by hydrogen bonds are centered at [n + 1/2, 1/2, 1/2] and [1/2, n + 1/2, 1/2] (n is zero or integer). These dimers are running along the a axis of the triclinic cell (Table 3 and Fig. 2a). In addition these dimers, the weak Cg…Cg (or π–π) interactions stabilize to crystal packing (Fig. 2b).

Geometry Optimization of (1)

In this work, we performed full geometry optimization of the title compound. Some selected geometric parameters experimentally obtained and theoretically calculated

Table 2. Selected geometrical parameters of the title compound with X-ray and DFT/B3LYP methods

	Experimental	B3LYP 6–311G**	B3LYP 6–31G**
Bond lengths (Å)			
S1–C13	1.721 (2)	1.753	1.754
S1–C14	1.731 (2)	1.758	1.761
N1–C12	1.397 (2)	1.386	1.389
N1–C14	1.302 (2)	1.298	1.302
N2–C14	1.360 (2)	1.369	1.369
N2–N3	1.373 (2)	1.350	1.353
N3–C15	1.268 (2)	1.287	1.282
N4–C16	1.352 (2)	1.376	1.378
N4–C19	1.367 (3)	1.367	1.368
Bond angles (°)			
C12–N1–C14	109.49 (14)	110.71	110.37
N1–C14–N2	124.54 (15)	122.58	122.63
C14–N2–N3	115.28 (14)	121.26	121.07
N2–N3–C15	117.94 (15)	118.31	118.15
N3–C15–C16	120.12 (16)	121.25	120.98
C16–N4–C19	108.51 (18)	109.91	109.90
Torsion angles (°)			
C9–C12–N1–C14	−176.92 (13)	−179.56	−179.66
C12–N1–C14–N2	179.55 (15)	179.84	179.83
N1–C14–N2–N3	172.67 (14)	179.43	179.47
C14–N2–N3–C15	166.25 (15)	179.49	179.31
C15–C16–N4–C19	−179.52 (17)	−179.92	−179.95

by B3LYP with 6–311G** and 6–31G** where ** is shown (d, p) as the basis sets are listed in Table 2. These calculated geometric parameters generally give bond lengths that are slightly larger than the experimental values, due to the fact that the theoretical calculations belong to isolated molecules in a gaseous phase and the experimental results belong to molecules in the solid state. It was found that both the bond lengths and the bond angles calculated by B3LYP methods are in good agreement with X-ray results. For example, the optimized bond lengths of N–C in thiazole and hydrazone groups fall in the range 1.287–1.386 Å for B3LYP/6-311G** and 1.282–1.389 Å for B3LYP/6–31G**, which is in good agreement with experimental bond lengths [1.268(2)–1.397(2) Å]. As can be seen in Table 2, theoretical calculations are in good agreement with each other as well as with experimental results.

Table 3. Hydrogen bond interaction of (**1**) (Å, °)

Hydrogen bond (Å, °)	D–H	H...A	D...A	D–H...A
N2–H2A...N1^i	0.86	2.20	3.058 (2)	176

Symmetry code: i: 1 – x, 1 – y, 1 – z.

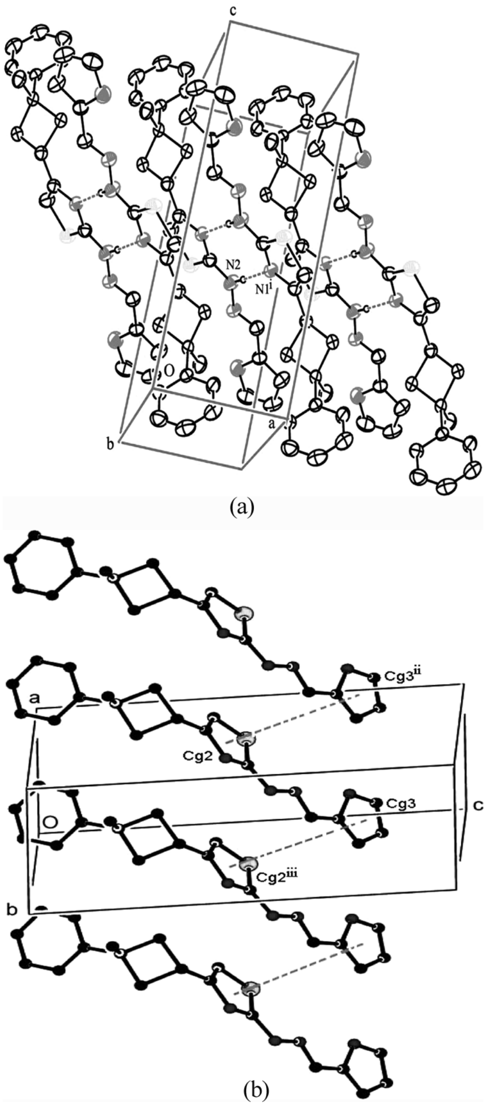

Figure 2. (a) A partial packing diagram for the compound, showing the N–H…N interaction as broken lines. Hydrogen atoms not involved in hydrogen bonding have been omitted. [Symmetry code: i: $1-x$, $1-y$, $1-z$]. (b) A partial packing diagram for the compound showing the Cg…Cg (or $\pi \ldots \pi$) interaction as broken lines. Hydrogen atoms not involved in interactions have been omitted (Cg2: thiazole ring, Cg3: pyrrol ring). Symmetry codes: ii: $1+x$, y, z, iii: $x-1$, y, z.

FTIR Spectra

Theoretical and experimental results of the title compound are shown in Table 4. No scale factor is used in the calculated frequencies. The experimental Fourier transform infrared (FTIR) spectrum is shown in Fig. 3. It is known that *ab initio* calculations systematically overestimate the vibrational wavenumbers and discrepancies.

Table 4. Vibrational frequencies of the title compound with X-ray and DFT/B3LYP methods

Frequencies	Experimental	B3LYP 6–311G**	B3LYP 6–31G**
ν(NH) pyr.	3,453	3,657	3,673
ν(NH) sch. base	3,171–2,854	3,511	3,529
ν_s(CH) pyr. + thi.	3,133	3,261–3,258	3,281–3,279
ν_{as}(CH) pyr. + thi.	3,066	3,244–3,232	3,264–3,251
ν_s(CH) phe.	3,021	3,186–3,175	3,204–3,192
ν_{as}(CH) phe.	2,965	3,168–3,154	3,175–3,171
ν_{as}(CH_2)	2,931	3,106–3,099	3,126–3,117
ν_{as}(CH_3)	2,854	3,087–3,085	3,111–3,108
ν_s(CH) sch. base	—	3,060	3,079
ν_s(CH_2) + ν_s(CH) cycl.	—	3,052–3,041	3,069–3,059
ν_s(CH_3) cycl.	—	3,019	3,035
ν(C=N)	1,613	1,669	1,685
ν(CC) phe.	—	1,645/1,621	1,660–1,636
δ(NH) + ν(C=N)	1,577	1,622	1,635
δ(NH) pyr. + ρ_t(CH)	1,536	1,588	1,603
ν(C=C) thi.	1,493	1,568	1,581
ρ_t(CH)	1,460	1,528	1,540
ρ_s(CH_2)	1,425	1,502	1,515
ρ_s(CH_3)	1,408	1,496–1,494	1,508
ρ_t(CH)+ ρ_s(CH_2)	1,354	1,475	1,507
δ(NH)+ ν(CCC)	1,277	1,429	1,475–1,421
ρ_t(CH) cycl.	1,238	1,394	1,401
δ(NH)+ δ(CH)	1,118	1,363	1,369
ν(NCN)	1,083	1,302	1,324–1,315
ν(CN)	1,036	1,290	1,298
t(CH_2)+t(CH_3)	1,009	1,173–1,169	1,265
ν(NN)+ ρ_t(CH)	964	1,164	1,177
ρ_s(CH)	921	1,054–1,032	1,063
δ(CH) out of plane	882	931	933
ν(CSC)	696	849	853
t(CH)	663	802–780	926
w(CH)	—	729–717	861
δ(NH) out of plane	—	681	680

Pyr: pyrrol, Sch. base: Schiff base, thi: thiazole, phe: phenyl, cycl: cyclobutane, υ: stretching, υ_s: symmetric stretching, υ_{as}: asymmetric stretching δ: bending, ρ_t: rocking, t: twisting, w: wagging, ρ_s: scissoring.

We noted that the experimental results belong to the solid phase and theoretical calculations belong to the gaseous phase. All the calculated spectra are in good agreement with the experimental data.

The characteristic υ(CH) stretching vibrations of heteroaromatic structures are expected to appear in 3,000–3,100 cm^{-1} frequency ranges [33,34]. In the present study, υ(CH) stretching vibrations of the title compound are observed at 3,133,

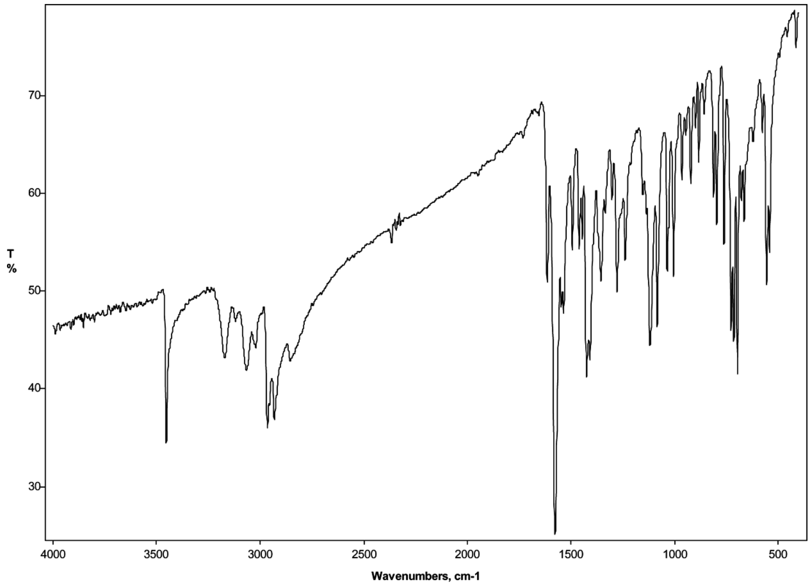

Figure 3. The experimental FTIR spectrum of the compound (**1**).

3,066, 3,021, and 2,965 cm^{-1}. Besides, the calculated bands at 1,536/1,460/1,354/1,238/964, 1,118, 921, 882, 663 cm^{-1} are attributed to five rocking, one bending, one scissorsing, one bending out of plane, and one wagging, which is in good agreement with the calculated frequencies for B3LYP method.

As shown in Table 4, experimentally determined vibrational bands of the compound were found to be significantly lower than calculated values; however, υ(NH) stretching vibrations are observed at 3,453–2,854 cm^{-1} and bending vibrations are observed at 1,577, 1,536, 1,277 and 1,118 cm^{-1} for experimental values. The formation of hydrogen bonds causes the significant low-wavelength shift and broadening of N–H stretching mode, and it can be observed around 2,500–3,500 cm^{-1} with multiple peaks. In this study, due to N2–H…N1 intermolecular hydrogen bonding, the N2–H stretching modes are observed at 2,854–3,171 cm^{-1} and it can be said that experimental υ(N2H) bending vibration increases, whereas υ(N2H) stretching vibration decreases [35]. In addition, as shown in Table 4, so many vibration species as symmetric, asymmetric stretching, twisting and scissorsing of CH_3 and CH_2 groups, stretching of C–N, C=N, C–C, C–S–C and N=C–N and other species are calculated with B3LYP/6-311G** and B3LYP/6–31G** methods and results of it are compared with experimental values.

The Mulliken charge distribution of the atoms in the compound is listed in Table 5. As can be seen from Table 5, the negative charges on the nitrogen atoms are significantly larger than the other atoms, but the positive charges are expected to be localized on the protonated nitrogen atoms. However, the calculations show that the positive charges are on hydrogens bound to the N2 and N4 atoms are found to be much different than those of other hydrogen atoms in the title compound, indicating that the positive charges are delocalized between the nitrogen and hydrogen atoms.

Table 5. Mulliken charges of some atoms of the title compound with DFT/B3LYP method

Atoms	B3LYP 6–311G**	B3LYP 6–31G**
N1	−0.36	−0.51
N2	−0.29	−0.39
H2A	0.22	0.27
N3	−0.22	−0.29
N4	−0.38	−0.55
H4A	0.24	0.28
C14	0.23	0.34
C15	0.13	0.11
H15	0.08	0.08
C16	0.12	0.28
C17	−0.15	−0.15
H17	0.09	0.08

Absorption Spectra

The calculations indicate that the compound has 89 occupied molecular orbitals (MOs). The HOMO energies, the LUMO energies, and the energy gap for the molecule mentioned above have been calculated by using B3LYP/6–311G** and B3LYP/6-31G** methods (see Table 6). An electronic system with a larger HOMO-LUMO gap should be less reactive than one having a smaller gap [36]. As shown in Table 6, the difference between HOMO and LUMO energy levels of the molecule is 3.918 eV for both the B3LYP/6-311G** method and B3LYP/6-31G** method.

The UV-Vis absorption spectra of the title compound were recorded in the $CHCl_3$ solutions. The compound exhibits absorption peaks in the UV-visible region. The absorption peaks are observed at 294 and 240 nm for the title compound. It can be said that these peaks are equal to $n \rightarrow \pi^*$ and $\pi \rightarrow \pi^*$ transitions. 3D plots of the HOMO-2, HOMO-1, HOMO, LUMO, LUMO+1, LUMO+2, and the corresponding energy levels for the title compound are shown in Fig. 4. The theoretical

Table 6. Molecular orbital energies of the title compound with DFT/B3LYP method

Energies	B3LYP 6–311G**	B3LYP 6–31G**
Homo (a.u.)	−0.192	−0.183
Lumo (a.u.)	−0.048	−0.039
Δ (a. u.) (eV)	0.144 (3.918)	0.144 (3.918)
Homo −1(a.u.)	−0.231	−0.222
Homo −2(a.u.)	−0.243	−0.234
Lumo +1 (a.u.)	−0.007	0.005
Lumo +2(a.u.)	−0.005	0.006

1 a.u. = 27.2116 eV.

electronic transfer (ET) peaks for the compound B3LYP/6-311G** and B3LYP/6-31G** basis sets are at 317, 247 and 317, 243 nm to correspond to the UV-Vis spectral absorption peaks, and the corresponding electronic transfers occurred between HOMO and LUMO, HOMO and LUMO+1, respectively. The greater theoretical absorption wavelengths of the compound have slight red shifts compared with the corresponding experimental ones.

Natural population analysis indicates that the electronic transitions are mainly derived from the contributions of bands $\pi \rightarrow \pi^*$ as reported in the literature [37]. As shown in Fig. 4, the electron clouds of the HOMO and HOMO-1 are delocalized on the thiazole and pyrrol rings connected with hydrazone bridge but the HOMO-2 s

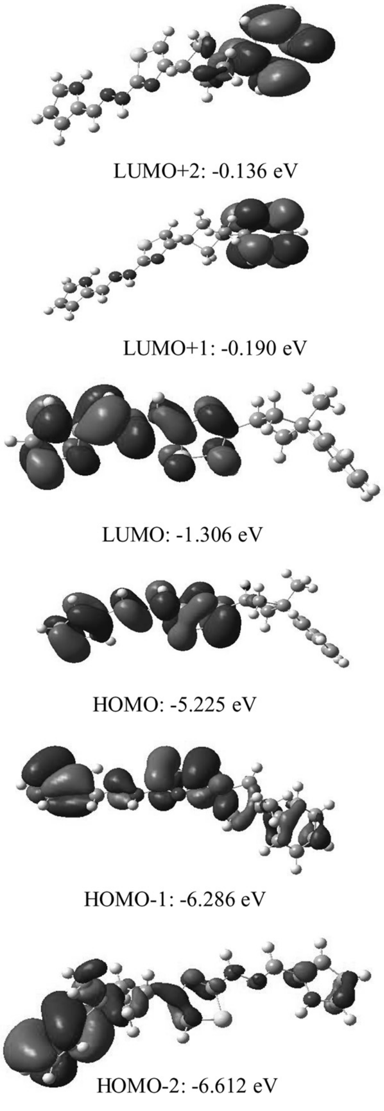

Figure 4. Plots of the frontier molecular orbitals of the compound (**1**) with DFT/B3LYP/6–311G** method.

are delocalized on phenyl ring. These orbitals appear to be the π-bonding type orbital. The electron cloud of the LUMO is mainly delocalized on thiazole, pyrrol rings, and hydrazone group, but it is found that LUMO+1 s and LUMO+2 s are mainly delocalized on the phenyl ring. In all cases, LUMOs are π^*-anti-bonding orbitals.

Molecular Electrostatic Potential

The molecular electrostatic potential (MEP) is related to the electronic density and is a very useful descriptor for determining sites for electrophilic attack and nucleophilic reactions as well as hydrogen-bonding interactions [38–40]. The electrostatic potential $V(r)$ is also well suited for analyzing processes based on the recognition of one molecule by another, as in drug–receptor and enzyme–substrate interactions, because it is through their potentials that the two species first "see" each other [41,42]. As a real physical property, $V(r)$ can be determined experimentally by diffraction or by computational methods [43].

To predict reactive sites for electrophilic and nucleophilic attacks for the title molecule, MEP was calculated at the B3LYP/6–311G** optimized geometry. The negative (red) regions of MEP were related to electrophilic reactivity and the positive (blue) regions to nucleophilic reactivity as shown in Fig. 5. As can be seen from the figure, there is a possible site on the title compound for electrophilic attack. The negative region is localized on the unprotonated nitrogen atom of the thiazole ring, N1, with a maximum value of −0.02801 a.u. However, a maximum positive region is localized on atom N2 probably due to the hydrogen, with a maximum value of 0.03801 a.u. This result provides information concerning the region where the compound can interact intermolecularly and bond covalently. Therefore, Fig. 5 confirms the existence of an intermolecular N–H…N interaction between the protonated and unprotonated N atoms of the thiazole ring and hydrazone group.

Thermodynamic Parameters of the Title Compound

Several thermodynamic parameters have been calculated using B3LYP/6-311G** and B3LYP/6-31G** levels and are given in Table 7. The total energies, zero-point

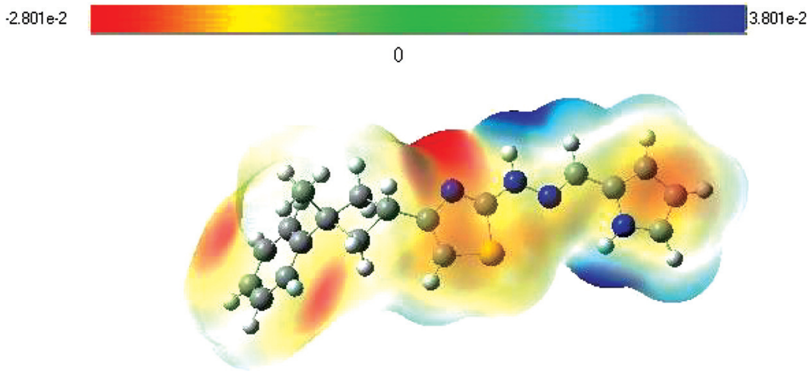

Figure 5. Molecular electrostatic potential map of the compound (**1**) with DFT/B3LYP/6–311G** method.

Table 7. Calculated energies (a.u), zero-point vibrational energies and enthalpies (kcal mol^{-1}), rotational constants (GHz), entropies and heat capacities (cal mol^{-1} K^{-1}), and dipole moment (D) for the title compound (**1**)

Parameters	B3LYP/6–311G**	B3LYP/6–31G**
Total energy (a.u.)	−1,353.461	−1,353.231
Dipole moment (D)	1.1807	1.1448
Zero-point vibrational energy	222.85247	224.05664
Rotational constants	0.65837	0.65394
	0.06270	0.06271
	0.06170	0.06173
Enthalpy (H)	14.190	14.159
Entropy (S)		
Translational	43.332	43.332
Rotational	36.088	36.094
Vibrational	84.267	83.246
Total	163.687	162.672
Heat capacity (C_v)		
Translational	2.981	2.981
Rotational	2.981	2.981
Vibrational	78.408	78.173
Total	84.370	84.134

vibrational energy (ZPVE), enthalpy (H(T)), entropy (S_{vib}(T)), and heat capacity (C_{vib}(T)) of the title compound at 298.15 K temperature and 1 atm pressure with different basis sets are presented. The zero point vibrational energy and total energy of the molecular structure are much lower by the B3LYP/6–311G** method than by the B3LYP/6–31G** method. They are 222.85247 and 224.05664 kcal.mol^{-1}, -1,353.461 and −1353.231 a.u. obtained at B3LYP/6–311G** and B3LYP/6–31G**, respectively. This values indicate that the title structure is quite stable. The dipole moment obtained at B3LYP/6–311G** level is the highest one (1.1807 D), and the value obtained at B3LYP/6–31G** level is 1.1448 D. The results of the energies, dipole moment, enthalpy, entropy, heat capacity, and ZPVE provide helpful information to further study the title compounds. They can be used to compute the other thermodynamic energies according to relationships of thermodynamic functions and estimate directions of chemical reactions according to the second law of thermodynamics in thermochemical fields.

Conclusions

The crystal structure of $C_{19}H_{20}N_4S$, (I), was investigated with X-ray diffraction and observed values of bond lengths and angles were compared with the calculated values. The theoretical vibrational spectrum assignments of $C_{27}H_{25}N_3S$, (I), were calculated and the experimental vibrational spectrum assignments of (I) were compared with theoretical results, In addition, the optimized molecular geometry, frontier molecular orbital properties, and Mulliken charge distribution of the atoms of this compound were calculated using *ab initio* calculations using density functional theory (DFT/B3LYP) with 6–311G** and 6–31G** basis sets. As a consequence, all the calculated spectra, and the optimized bond lengths and angles are in good agreement with the experimental results. As mentioned in the Introduction, this compound has been synthesized as a part of our ongoing research program. According to the observed results, there is a good relationship between the results of the present study and expected functionalities from the structure of the molecule.

Supplementary Data

Crystallographic data for the structural analysis have been deposited with the Cambridge Crystallographic Data Centre, CCDC No 748347. Copies of this information may be obtained free of charge from the Director, CCDC, 12 Union Road, Cambridge CB2 1EZ, UK (fax: +44–1223-336033; e-mail: deposit@ccdc.cam.ac.uk or :http://www.ccdc.cam.ac.uk).

Acknowledgment

The authors acknowledge the Faculty of Arts and Sciences, Ondokuz Mayis University, Turkey, for the use of the STOE IPDS-II diffractometer (purchased under grant F.279 of the University Research Fund).

References

[1] Tarafder, M. T. H., Jin, K. T., Crouse, K. A., Ali, A. M., Yamin, B. M. & Fun, H.-K. (2002). *Polyhedron*, *21*, 2547.

[2] Guerriero, P., Tamburini, S. & Vigato, P. A. (1995). *Coord. Chem. Rev.*, *139*, 17.

[3] Sreekala, R. & Yusuff, K. K. M. (1992). *React. Kinet. Catal. Lett.*, *48*, 575.

[4] Das, N. N. & Dash, A. C. (1995). *Polyhedron*, *14*, 1221.

[5] Williams, D. R. (1972). *Chem. Rev.*, *72*, 203.

[6] Tsapkov, V. I. (2002). *Russ. J. Gen. Chem.*, *72*, 276.

[7] Ghosh, S. & Bandyopadhyay, T. K. (1985). *Trans., Met. Chem.*, *10*, 57.

[8] Shan, S., Xu, D.-J., Wu, J.- Y. & Chiang, M. Y. (2002). *Acta Crystallograph.*, *E58*, o1444.

[9] Bosan, W. S., Shank, R. C., MacEwen, J. D., Gaworski, C. L. & Newberne, P. M. (1987). *Carcinogenesis*, *8*, 439.

[10] Roberge, A., Gosslin, C. & Charbonneau, R. (1971). *Biochem. Pharmacol.*, *20*, 2231.

[11] Waterfield, C. J., Asker, D. S. & Timbrell, J. A. (1997). *Chem. Biol. Int.*, *107*, 157.

[12] Rothgery, E. F. (2005). *Kirk-Othmer Encyclopedia of Chemical Technology*, Wiley-InterScience: New York.

[13] Schmidt, E. W. (2001). *Hydrazine and Its Derivatives: Preparation, Properties, Applications*, Wiley: Chichester, UK.

[14] Tezcan, H., Tunç, T., Şahin, E. & Yagbasan, R. (2004). *Anal. Sci.*, *20*, x137.

[15] Townshend, A. & Wheatly, R. A. (1998). *Analysis*, *123*, 1041.

[16] Saprykina, V. A., Vinogradova, V. I., Ambartsumova, R. F., Ibragimov, T. F. & Shakhidoyatov, Kh. M. (2006). *Chem. Nat. Comp.*, *42*, 4470.

[17] Hadjipavlou-Litina, J. D. & Geronikaki, A. (1996). *Arzneim Forsch/ Drug Res.*, *46*, 805.

[18] Holla, B. S., Malini, K. V., Rao, B. S., Sarojini, B. K. & Kunari, N. S. (2003). *Eur. J. Med. Chem.*, *38*, 313.

[19] Cukurovali, A., Yilmaz, I., Gur, S. & Kazaz, C. (2006). *Eur. J. Med. Chem.*, *41*, 201.

[20] Sheldrick, G. M. (1997). *SHELXS-97 and SHELXL-97*, University of Gottingen: Germany.

[21] Farrugia, L. J. (1997). *J. Appl. Cryst.*, *30*, 565.

[22] Spek, A. L. (2003). *J. Appl. Cryst.*, *36*, 7.

[23] Becke, A. D. (1993). *J. Chem. Phys.*, *98*, 5648.

[24] Lee, C., Yang, W., & Parr, R. G. (1988). *Phys. Rev.*, *B37*, 785.

[25] Frish, A., Nielseni, A. B. & Holder, A. J. (2001). *Gaussview User Manual*, Gaussian Inc.: Pittsburg, PA.

[26] Frisch, M. J., Trucks, G. W., Schlegel, H. B., Scuseria, G. E., Robb, M. A., Cheeseman, J. R., Montgomery, J. A., Vreven, T., Kudin, K. N., Burant, J. C., Millam, J. M., Iyengar, S. S., Tomasi, J., Barone, V., Mennucci, B., Cossi, M., Scalmani, G., Rega, N., Petersson, G. A., Nakatsuji, H., Hada, M., Ehara, M., Toyota, K., Fukuda, R., Hasegawa, J., Ishida, M., Nakajima, T., Honda, Y., Kitao, O., Nakai, H., Klene, M., Li, X., Knox, J. E., Hratchian, H. P., Cross, J. B., Adamo, C., Jaramillo, J., Gomperts, R., Stratmann, R. E., Yazyev, O., Austin, A. J., Cammi, R., Pomelli, C., Ochterski, J. W., Ayala, P. Y., Morokuma, K., Voth, G. A., Salvador, P., Dannenberg, J. J., Zakrzewski, V. G., Dapprich, S., Daniels, A. D., Strain, M. C., Farkas, O., Malick, D. K., Rabuck, A. D., Raghavachari, K., Foresman, J. B., Ortiz, J. V., Cui, Q., Baboul, A. G., Clifford, S., Cioslowski, J., Stefanov, B. B., Liu, G., Liashenko, A., Piskorz, P., Komaromi, I., Martin, R., Fox, D. J., Keith, T., Al-Laham, M. A., Peng, C. Y., Nanayakkara, A., Challacombe, M., Gill, P. M. W., Johnson, B., Chen, W., Wong, M. W., Gonzalez, C., & Pople, J. A. (2004). *Gaussian 03*, Gaussian, Inc.: Wallingford, CT.

[27] Allen, F. H. (1984). *Acta Cryst.*, *E40*, 64.

[28] Yüksektepe, Ç., Çalışkan, N., Yılmaz, I. & Çukurovali, A. (2006). *Acta Cryst.*, *E62*, o2762.

[29] Liu, G., Liu, L., Jia, D., & Yu, K. (2005). *J. Chem. Cryst.*, *35*, 497.

[30] Ma, Q., Lu, L.-P., & Zhu, M.-L. (2008). *Acta Crystallograph.*, *E64*, o2026.

[31] Yüksektepe, Ç., Saraçoğlu, H., Koca, M., Çukurovali, A. & Çalışkan, N. (2004). *Acta Crystallograph.*, *C60*, o509.

[32] Yüksektepe, Ç., Soylu, M. S., Saraçoğlu, H., Yılmaz, I., Çukurovali, A. & Çalışkan, N. (2005). *Acta Cryst.*, *E61*, o1158.

[33] Arslan, H. & Algül, Ö. (2007). *Int. J. Mol. Sci.*, *8*, 760.

[34] Siddiqui, S. A., Dwivedi, A., Singh, P. K., Hasan, T., Jain, S., Prasad, O. & Misra, N. (2009). *J. Struc. Chem.*, *50*, 411.

[35] Silverstein, R. M., Bassler, G. C. & Morrill, T. C. (1963). *Spectrometric Identification of Organic Compounds*, John Wiley & Sons: New York.

[36] Kurtaran, R., Odabaşoğlu, S., Azizoğlu, A., Kara, H. & Atakol, O. (2007). *Polyhedron*, *26*, 5069.

[37] Sun, Y.-X., Wei, W.-X., Hao, Q.-L., Lu, L.-D. & Wang, X. (2009). *Spectrochin. Acta*, *A73*, 772.

[38] Scrocco, E., & Tomasi, J. (1979). *Adv. Quant. Chem.*, *11*, 115.

[39] Luque, F. J., Lopez, J. M., & Orozco, M. (2000). *Theor. Chem. Accounts*, *103*, 343.

[40] Okulik, N. & Jubert, A. H. (2005). *Internet Electron. J. Mol. Des.*, *4*, 17.

[41] Politzer, P., Laurence, P. R., & Jayasuriya, K. (1985). *Environ. Health Perspect.* [special issue], *61*, 191.

[42] Scrocco, E., & Tomasi, J. (1973). *Topics in Current Chemistry*, Springer: Berlin.

[43] Politzer, P., & Truhlar, D. G. (1981). *Chemical Applications of Atomic and Molecular Electrostatic Potentials*, Plenum: New York.